IOP Publishing Journal of Physics G: Nuclear and Particle Physics

J. Phys. G: Nucl. Part. Phys. **50** (2023) 105002 (20pp) https://doi.org/10.1088/1361-6471/ace3df

Probe of axion-like particles in vector boson scattering at a muon collider

S C İnan[1,*] and A V Kisselev[2]

[1] Department of Physics, Sivas Cumhuriyet University, 58140, Sivas, Turkey
[2] A.A. Logunov Institute for High Energy Physics, NRC 'Kurchatov Institute', 142281, Protvino, Russia

E-mail: sceminan@cumhuriyet.edu.tr and alexandre.kisselev@ihep.ru

Received 19 December 2022, revised 26 May 2023
Accepted for publication 4 July 2023
Published 5 September 2023

Abstract

We have examined the sensitivity of the axion-like particles (ALP) couplings to electroweak gauge bosons in the diphoton production at a future muon collider. The collisions at the $\mu^+\mu^-$ energies of 3 TeV, 14 TeV, and 100 TeV are addressed. The differential cross sections versus the invariant mass of the final photons and total cross section versus minimal diphoton invariant mass are presented. We have derived the exclusion regions for the ALP-gauge boson coupling. The obtained bounds are much stronger than the current experimental bounds in the ALP mass region 10 GeV to 10 TeV. The partial-wave unitarity constraints on the ALP-gauge boson coupling are estimated. We have shown that the unitarity is not violated in the region of the ALP coupling studied in the present paper.

Keywords: axion-like particles, gauge bosons, muon collider

(Some figures may appear in colour only in the online journal)

1. Introduction

The strong CP problem of the Standard Model (SM) can be solved by introducing a spontaneously broken Peccei–Quinn symmetry [1, 2]. As a result, a light pseudo-Nambu–Goldstone boson, QCD axion, arises [3, 4]. The QCD axion is a well-motivated candidate for the DM [5–9] which can be produced via the vacuum misalignment mechanism [5, 10] or as the decay of topological defects [11].

The axion-like particles (ALPs) are particles having interactions similar to the axion. The origin of the ALP is expected to be similar but without the relationship between its coupling

[*] Author to whom correspondence should be addressed.

constant and mass. It means that the ALP mass can be treated independently of its couplings to the SM fields. Since the ALPs are not directly relevant for the QCD axion, heavy ALPs can be detected at colliders. The production of the ALPs was studied in the *pp* [12–19] and heavy-ion [13, 18, 20–22] collisions at the LHC, as well as at future colliders [23–31], including electron-ion scattering [32, 33]. For a review on the axions and ALPs, see [9, 34–39] and references therein.

Many ALP searches assume their strong couplings to the electromagnetic term $F_{\mu\nu}\tilde{F}^{\mu\nu}$. One of the most preferred processes to probe the ALP-photon coupling is a light-by-light (LBL) scattering. The first evidence of the subprocess $\gamma\gamma \to \gamma\gamma$ was observed by the ATLAS and CMS collaborations in high-energy ultra-peripheral PbPb collisions [40–42]. The phenomenology of the LBL scattering at the LHC was examined in [43–47]. In a number of papers [24, 25, 48, 49] a phenomenology of the LBL collisions at future e^+e^- colliders were presented. The search for ALPs in the $\gamma\gamma \to a \to \gamma\gamma$ collision with proton tagging at the LHC was given in [12].

It is a muon collider that could provide the simplest, but the most striking signature of the existence of the ALPs [50–53]. Muon colliders were proposed by Tikhonin and Budker in the late 1960's [54, 55]. Then they were actively discussed in the early 1980s [56, 57]. Muon colliders have a great potential for high-energy physics since they can offer collisions of elementary particles at very high energies. The point is that muons can be accelerated in a ring without limitation from synchrotron radiation compared to linear or circular electron-positron colliders [58–60]. Note, however, that getting high luminosity needs to solve a technical problem related to the short muon lifetime at rest and the difficulty of producing large numbers of muons in bunches with small emittance [61–64].

Note that muon collider has a low level of beamstrahlung and synchrotron radiation compared to linear or circular electron-positron colliders. As a result, it enables reduced energy spread in the collision and an improved energy resolution. That is why, the muon collider is the ideal machine to collide elementary particles at high energies and luminosities [65, 66].

The muon collider could provide a determination of the electroweak couplings of the Higgs boson which is significantly better than what is considered attainable at other future colliders [67–73]. Interest in designing and building a muon collider is also based on its capability of probing the physics beyond the SM. In a number of recent papers searches for SUSY particles [74], WIMPs [75], vector boson fusion [76], leptoquarks [77], lepton flavor violation [78], and physics of $(g-2)_\mu$ [79] at the muon colliders are presented.

In the present paper, we study the high-energy production of the ALP in the $\mu^+\mu^- \to \mu^+\gamma\gamma\mu^-$ process which goes via vector boson fusion subprocess $V_1V_2 \to a \to \gamma\gamma$, where $V_{1,2}$ is γ or Z, and a is a heavy ALP. The main goal is to obtain constraints on the ALP-vector boson coupling as a function of the ALP mass at TeV and multi-TeV muon colliders.

2. ALP in gauge boson scattering

The interaction of the ALP a with SM gauge bosons is described by the Lagrangian

$$\mathcal{L}_{\text{int}} = \frac{1}{2}\,\partial_\mu a\,\partial^\mu a - \frac{1}{2}m_a^2 a^2 + g^2 C_{BB}\frac{a}{\Lambda}B_{\mu\nu}\tilde{B}^{\mu\nu} + g'^2 C_{WW}\frac{a}{\Lambda}W_{\mu\nu}^c\tilde{W}^{c,\mu\nu}, \tag{1}$$

where $B_{\mu\nu}$ and $W_{\mu\nu}^c$ are the field strength of $U(1)_Y$ and $SU(2)_L$, respectively, while $\tilde{B}_{\mu\nu}$ and $\tilde{W}_{\mu\nu}^c$ are dual field strength tensors. As was already mentioned above, the ALP mass m_a and coupling f_a can be regarded as independent parameters. After electroweak symmetry breaking, the ALP couples to the photon and Z boson as

$$\mathcal{L}_a = \frac{1}{2}\,\partial_\mu a\,\partial^{\,\mu} a - \frac{1}{2} m_a^2 a^2 + g_{a\gamma\gamma} a F_{\mu\nu}\tilde{F}^{\mu\nu} + g_{a\gamma Z} a F_{\mu\nu}\tilde{Z}^{\mu\nu} + g_{aZZ} a Z_{\mu\nu}\tilde{Z}^{\mu\nu}, \tag{2}$$

Here $\tilde{F}_{\mu\nu} = (1/2)\varepsilon_{\mu\nu\alpha\beta}F_{\alpha\beta}$ and $\tilde{Z}_{\mu\nu} = (1/2)\varepsilon_{\mu\nu\alpha\beta}Z_{\alpha\beta}$ are the dual tensors, and

$$\begin{aligned} g_{a\gamma\gamma} &= \frac{e^2}{\Lambda}[C_{WW} + C_{BB}], \\ g_{a\gamma Z} &= \frac{2e^2}{\Lambda s_w c_w}[c_w^2 C_{WW} - s_w^2 C_{BB}], \\ g_{aZZ} &= \frac{e^2}{\Lambda s_w^2 c_w^2}[c_w^4 C_{WW} + s_w^4 C_{BB}], \end{aligned} \tag{3}$$

where s_w and c_w are sine and cosine of the Weinberg angle, respectively.

In what follows, we assume that the ALP couples to hypercharge $U(1)_Y$, not to $SU(2)_L$, that corresponds to $C_{WW} = 0$. Let us define $e^2 C_{BB}/\Lambda = 1/f_a$, then a set of the ALP couplings takes the form

$$g_{a\gamma\gamma} = \frac{1}{f_a}, \quad g_{a\gamma Z} = -\frac{2s_w}{c_w}\frac{1}{f_a}, \quad g_{aZZ} = \frac{s_w^2}{c_w^2}\frac{1}{f_a}. \tag{4}$$

We also assume that the ALP has a non-zero total width

$$\Gamma_a = \frac{\Gamma(a \to \gamma\gamma)}{\mathrm{Br}(a \to \gamma\gamma)}, \tag{5}$$

where

$$\Gamma(a \to \gamma\gamma) = \frac{m_a^3}{4\pi f_a^2} \tag{6}$$

is the ALP decay width into two photons. In general, the ALP can also couple to fermions as $\partial^\mu a \bar{\psi}\gamma_\mu\gamma_5\psi$. But for $m_a \gg m_\psi$ the full width of the ALP decay should be mainly defined by its decay to two photons. In our upcoming calculations the ALP branching $\mathrm{Br}(a \to \gamma\gamma)$ is considered as a free parameter that is equal to (or less than) 1.

The differential cross section of the subprocess $V_1 V_2 \to \gamma\gamma$, where $V_{1,2} = \gamma, Z$, is a sum of helicity amplitudes squared

$$\frac{\mathrm{d}\hat{\sigma}}{\mathrm{d}\Omega}(\lambda_1\lambda_2) = \frac{1}{64\pi^2\hat{s}}\sum_{\lambda_3,\lambda_4}|M_{\lambda_1\lambda_2\lambda_3\lambda_4}|^2, \tag{7}$$

where $\sqrt{\hat{s}}$ is a collision energy of this subprocess, and λ_3, λ_4 are helicities of the outgoing photons. In its turn, each of the helicity amplitudes in (7) is a sum of the ALP and SM (electroweak) terms

$$M = M_a + M_{\mathrm{ew}}. \tag{8}$$

The Feynman diagrams describing M_a are shown in figure 1. The explicit expressions of the ALP helicity amplitudes of the $\gamma\gamma \to \gamma\gamma$ process can be found in [12] (see also [24]). The results of our calculations of the ALP helicity amplitudes M_a of the processes $Z\gamma \to \gamma\gamma$ and $ZZ \to \gamma\gamma$ are presented in appendix. Each of the SM amplitudes is a sum of the fermion and W boson one-loop amplitudes

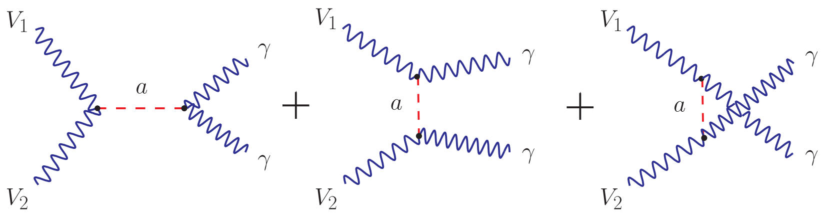

Figure 1. The Feynman diagrams describing virtual production of the axion-like particle a in the collision of two vector bosons V_1, $V_2 = \gamma$ or Z, with two outgoing photons.

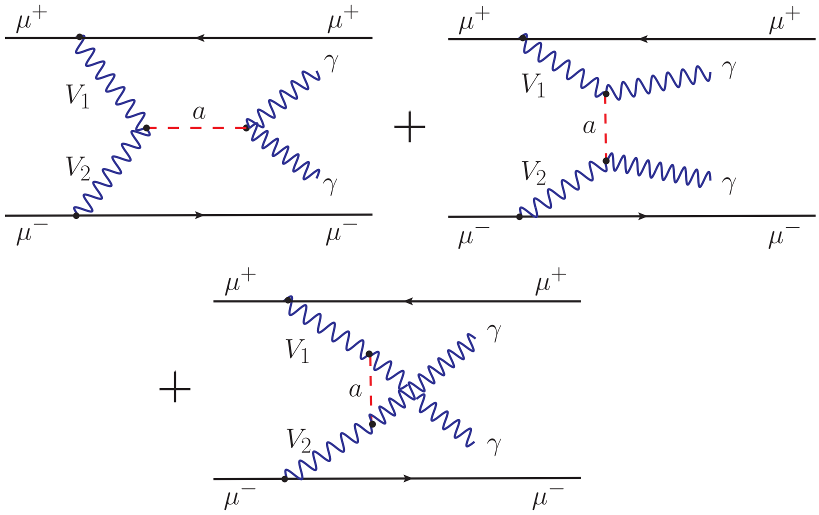

Figure 2. The Feynman diagrams describing virtual production of the axion-like particle a in the $\mu^+\mu^-$ collision via vector boson fusion.

$$M_{\mathrm{ew}} = M_{\mathrm{ew}}^f + M_{\mathrm{ew}}^W. \tag{9}$$

The SM helicity amplitudes M_{ew}^f and M_{ew}^W have been calculated for the processes $\gamma\gamma \to \gamma\gamma$ [80–82] (see also [83]), $\gamma\gamma \to \gamma Z$ [84], and $\gamma\gamma \to ZZ$ [85].

2.1. Differential cross section of diphoton production

We consider the process shown in figure 2. In the equivalent photon approximation (EPA) [86–91], we have the following leading logarithmic approximation distributions for the photon with the helicities $+1$ and -1 in *unpolarized* fermion beam ($f = \mu^-$, in our case) [90]

$$f_{\gamma_\pm/f}(x, Q^2) = f_{\gamma/f}(x, Q^2) = \frac{\alpha}{4\pi}\frac{1 + (1 - x)^2}{x} \ln\frac{Q^2}{m_\mu^2}, \tag{10}$$

where $x = E_\gamma/E_\mu$ is the ratio of the photon energy E_γ and energy of the incoming muon E_μ, m_μ is the muon mass. Note that due to C and P invariances, $f_{\gamma/\bar{f}} = f_{\gamma/f}$, where $\bar{f}$ denotes anti-fermion (μ^+, in our case).

To examine the collisions of massive vector bosons ($W^\pm$ and Z), the effective W approximation (EWA) is applied [92, 93] which allows to treat massive vector bosons as partons inside the colliding beams (see also [94–102]). In this scheme, the Z boson has different distributions for its transverse (±1) and longitudinal (0) polarizations. The leading order distributions of the Z boson in *unpolarized* fermion beam are the following [76, 99, 102]

$$f_{Z_\pm/f}(x, Q^2) = \frac{\alpha_Z}{4\pi}\frac{(g_V^f \mp g_A^f)^2 + (g_V^f \pm g_A^f)^2(1-x)^2}{x}\ln\frac{Q^2}{m_Z^2},$$
$$f_{Z_0/f}(x, Q^2) = \frac{\alpha_Z}{\pi}\frac{[(g_V^f)^2 + (g_A^f)^2](1-x)}{x}, \tag{11}$$

where

$$\alpha_Z = \frac{\alpha}{(\cos\theta_W \sin\theta_W)^2}, \tag{12}$$

and

$$g_V^f = \frac{1}{2}(T_3^f)_L - Q^f \sin^2\theta_W, \quad g_A^f = -\frac{1}{2}(T_3^f)_L. \tag{13}$$

The PDFs of anti-fermions are related to those of fermions by CP relation, $f_{Z_\pm/\bar{f}} = f_{Z_\mp/f}$. Note that both EPA and EWA are an inclusive description. No cuts are imposed on the outgoing muons.

The cross section of our process $\mu^-\mu^+ \to \mu^- V_1 V_2 \mu^+ \to \mu^-\gamma\gamma\mu^+$ is defined by the formula

$$d\sigma = \int_{\tau_{\min}}^{\tau_{\max}} d\tau \int_{x_{\min}}^{x_{\max}} \frac{dx}{x} \sum_{V_1, V_2} f_{V_1/\mu^+}(x, Q^2) f_{V_2/\mu^-}(\tau/x, Q^2)\, d\hat{\sigma}(V_1 V_2 \to \gamma\gamma), \tag{14}$$

where $V_{1,2}$ runs $\gamma_+, \gamma_-, Z_+, Z_-, Z_0$

$$x_{\max} = 1 - \frac{m_\mu}{E_\mu},\ \tau_{\max} = \left(1 - \frac{m_\mu}{E_\mu}\right)^2,\ x_{\min} = \tau/x_{\max},\quad \tau_{\min} = \frac{p_\perp^2}{E_\mu^2}, \tag{15}$$

and $p_\perp$ is the transverse momenta of the outgoing photons. The boson distributions inside the muon beam, $f_{\gamma_\pm/\mu^\pm}(x, Q^2)$, $f_{Z_\pm/\mu^\pm}(x, Q^2)$, and $f_{Z_0/\mu^\pm}(x, Q^2)$ are given by equations (10) and (11), respectively, and the subprocess cross section $d\hat{\sigma}(V_1V_2 \to \gamma\gamma)$ is defined by equation (7). We take $Q^2 = \hat{s}$, where $\sqrt{\hat{s}} = 2E_\mu\sqrt{\tau}$ is the invariant energy of the VBF subprocess $V_1V_2 \to \gamma\gamma$.

2.2. Numerical analysis

Since the ALP mass and couplings can be treated independently, it is not surprising that heavy ALPs, with masses up to a few TeV, were searched for at the LHC (see, for instance, figure 4 in [23]). In the present section, we will examine the production of heavy ALPs in the 10 GeV to 10 TeV mass region.

The results of our calculations of the differential cross section for the $\mu^+\mu^- \to \mu^+\gamma\gamma\mu^-$ collision at the future muon collider are presented in figure 3 as a function of the invariant mass of the detected photons $m_{\gamma\gamma}$. The collision energies $\sqrt{s}$ of 3 TeV, 14 TeV and 100 TeV, and two values of the ALP branching Br(a $\to \gamma\gamma$) are addressed. The ALP mass is taken to be equal to $m_a = 1$ TeV. The ALP-boson couplings f_a are chosen to be equal to 5 TeV, 10 TeV, and 50 TeV for the left, middle, and right panels, respectively. The sharp peaks for $\sqrt{s} = 3$ TeV and $\sqrt{s} = 14$ TeV are the resonance peaks located at $m_{\gamma\gamma} = 1$ TeV. They are more pronounced for larger Br(a $\to \gamma\gamma$).

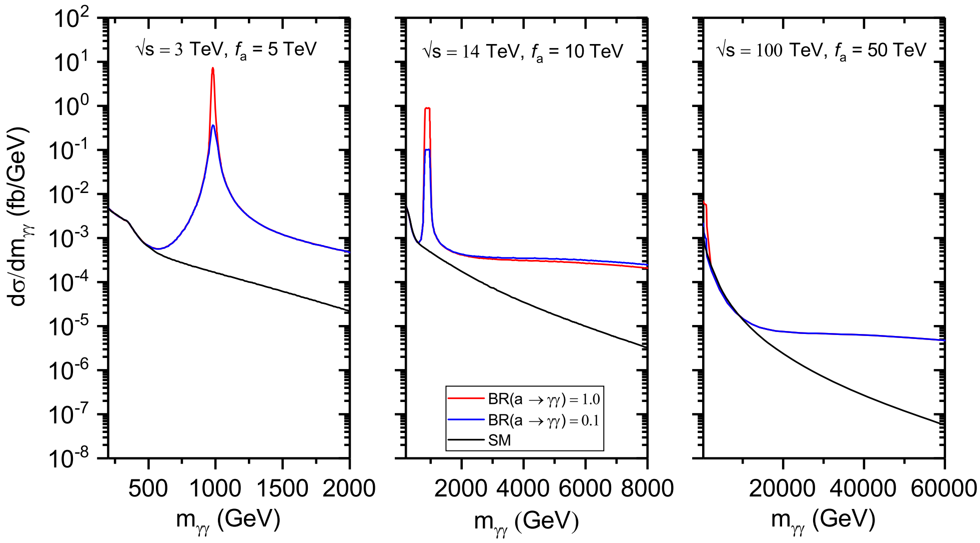

Figure 3. The differential cross sections for the $\mu^+\mu^- \to \mu^+\gamma\gamma\mu^-$ scattering at the future muon collider versus diphoton invariant mass $m_{\gamma\gamma}$. The curves correspond to the ALP mass $m_a = 1$ TeV. The ALP-gauge boson coupling f_a is equal to 5 TeV, 10 TeV, and 50 TeV for the center-of-mass energy 3 TeV, 14 TeV, and 100 TeV, respectively.

The dominant background is the SM process $\mu^+\mu^- \to \gamma\gamma$, the continuous background is $\mu^+\mu^- \to \mu^+\gamma\gamma\mu^-$ [53]. As was already mentioned in Introduction, the muon collider has a reduced initial-state-radiation (ISR), contrary to e^+e^- collider. We expect that the tail of the beam energy spread is not large. To suppress a sizable contribution of the large cross section of $\mu^+\mu^- \to \gamma\gamma$ to a background rate, we impose a strong upper cut on the diphoton invariant mass, $m_{\gamma\gamma} < m_{\gamma\gamma,\max} = 0.9\sqrt{s}$. The ISR effects of the future muon colliders have been studied, for instance, in [103]. As one can see in figure 1 in [103], the beam energy distribution decreases exponentially as a function of the energy fraction $x = \sqrt{\hat{s}/s}$ from the ISR effects ($\hat{s} = m_{\gamma\gamma}^2$ in our case). For $x < 0.9$ we get the large suppression factor $\exp(-(1-x)/R)$, where R is the beam energy resolution ($R = 0.01(0.003)\%$ for future muon colliders).[3] Thus, our cut is sufficient to suppress the main background. The resulting SM background is shown in figure 3. One can see that a discrepancy between the cross section and its SM part becomes significant as $m_{\gamma\gamma}$ grows.

In figure 4 we present the total cross section $\sigma(m_{\gamma\gamma,\min} < m_{\gamma\gamma} < m_{\gamma\gamma,\max})$, where $m_{\gamma\gamma,\min}$ is the minimal invariant mass of the final photons $m_{\gamma\gamma}$, and $m_{\gamma\gamma,\max}$ is defined above. As one can see from figure 3, the main contribution to the total cross sections comes from the region $m_{\gamma\gamma} \ll m_{\gamma\gamma,\max}$ because of the resonance-like behavior of the differential cross section. Moreover, our calculations show that the differential cross section gets very small as $m_{\gamma\gamma}$ approaches $\sqrt{s}$. In the region $m_{\gamma\gamma,\min} < 1000$ GeV, the new physics cross section do not change for all $\sqrt{s}$. For $m_{\gamma\gamma,\min} > 1000$ GeV, the deviation of the cross-section from its SM part is very large. Moreover, for $\sqrt{s} = 14$ TeV and $\sqrt{s} = 100$ TeV it gets larger and larger as $m_{\gamma\gamma,\min}$ grows. In our calculations, we also apply the cuts on the rapidity and transverse momentum of the outgoing photons, $|\eta| < 2.5$ and $p_t > 30$ GeV, respectively.

[3] It is not the case for the *resonance* Higgs production when $s \simeq \hat{s} = m_h^2$ [103].

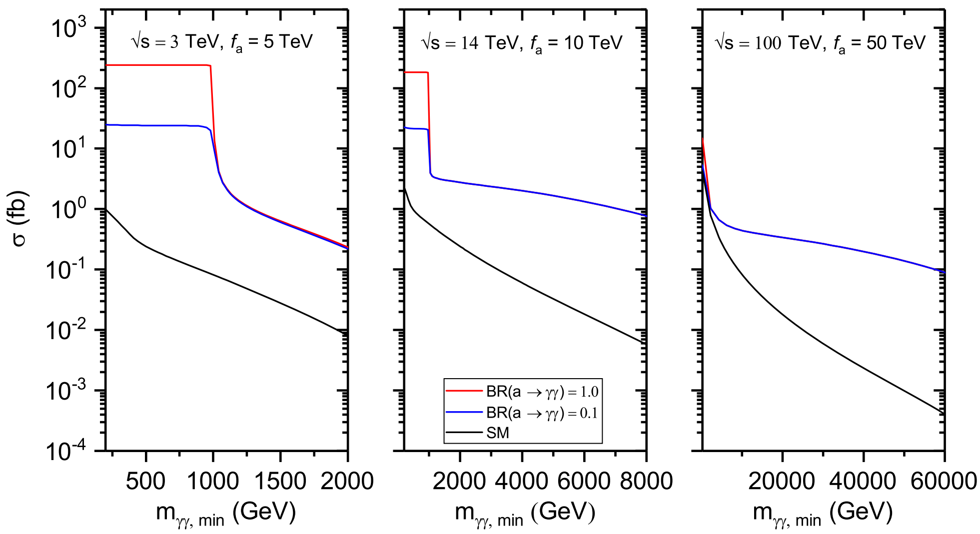

Figure 4. The total cross sections $\sigma(m_{\gamma\gamma,\min} < m_{\gamma\gamma} < m_{\gamma\gamma,\max})$ for the $\mu^+\mu^- \to \mu^+\gamma\gamma\mu^-$ scattering at the future muon collider versus minimal value of the diphoton invariant mass $m_{\gamma\gamma}$. The values of the ALP mass m_a and ALP-gauge boson coupling f_a are the same as in figure 3.

To derive the exclusion region, we apply the following formula for the statistical significance SS [104]

$$SS = \sqrt{2[(S - B\,\ln(1 + S/B)]}\,, \tag{16}$$

where S is the number of signal events and B is the number of background (SM) events. We define the regions $SS \leqslant 1.645$ as the regions that can be excluded at the 95% C.L. To reduce the SM background, we used the additional cut $m_{\gamma\gamma} > 800$ GeV. All our cuts improve significantly signal-to-background ratio. The results are shown in figure 5. Following [62] (see also [75]), we consider the integrated luminosities of 1 ab^{-1}, 20 ab^{-1}, and 1000 ab^{-1} for the muon collider energies of 3 TeV, 14 TeV, and 100 TeV, respectively.

As one can see in figure 5, for $\sqrt{s}\, = 3$ TeV the best sensitivity region is limited to a rather sharp region 800 GeV—2 TeV. In this region, the ALP term dominates, while outside it the contributions from the ALP and SM terms are comparable and they partially cancel each other. For $\sqrt{s}\, = 14$ TeV and $\sqrt{s}\, = 100$ TeV the ALP contributions dominate in wider regions of the ALP mass ($\geqslant$800 GeV). The best bounds for 14 and 100 TeV are those seen on the figure, and for larger mass region the bounds become weaker. A similar effect was shown to take place for the ALP production in the LBL scattering [24] (for details, see appendix in [24]). The best limits corresponds to $\mathrm{Br}(a \to \gamma\gamma) = 1$. The unitary limits are also shown. For comparison, in figure 6 we present previously obtained 95% C.L. exclusion region for the ALP-photon coupling coming from the polarized LBL scattering at the 3 TeV CLIC [24]. Other current exclusion regions for this coupling are also shown [12]. As seen from figures 5 and 6, the excluded areas that we have found from studying diphoton production at the muon collider extends to wider regions, especially for $\sqrt{s}\, = 14$ TeV and $\sqrt{s}\, = 100$ TeV.

In the present paper, we have assumed that the ALP to couple only to hypercharge $U(1)_Y$. The same assumption ($C_{WW} = 0$) was used in [23], where the bound $f_a^{-1} < 0.05$ TeV^{-1} was derived for 100 TeV FCC-hh. As was pointed out in [105], for light ALPs there are strong

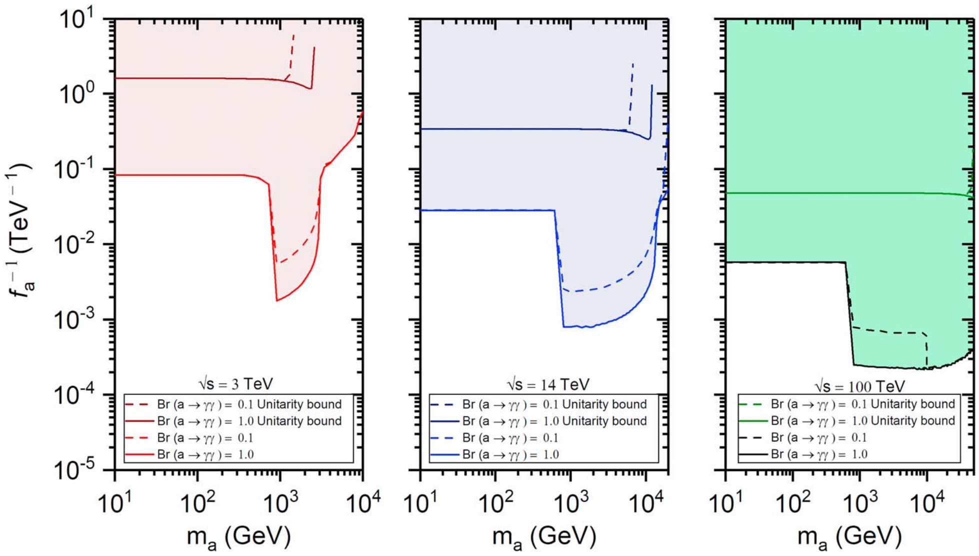

Figure 5. 95% C.L. exclusion regions for the ALP-gauge boson coupling f_a coming from the $\mu^+\mu^- \to \mu^+\gamma\gamma\mu^-$ scattering at the future muon collider. The curves are obtained with the use of the cut on diphoton invariant mass, $m_{\gamma\gamma} > 800$ GeV. The unitary bounds are also shown.

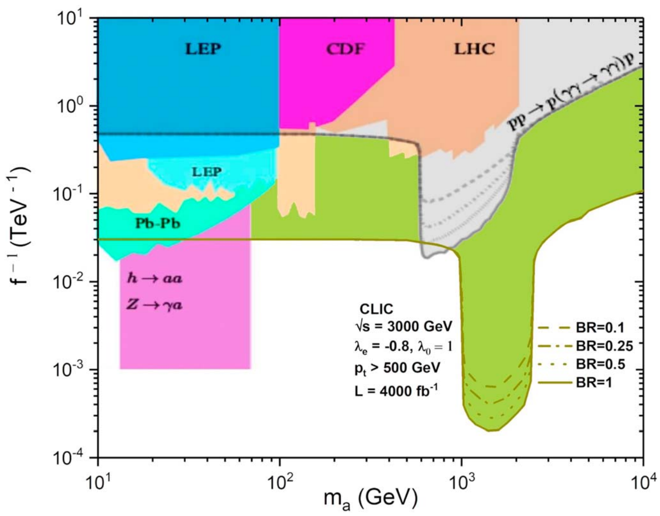

Figure 6. Our previous 95% C.L. exclusion region for the ALP-photon coupling in the polarized light-by-light scattering at the 3 TeV CLIC induced by ALPs (green area) [24] in comparison with other current exclusion regions [12].

constraints on C_{WW} from loop-induced flavor-changing processes. To simplify the analysis in a number of papers different assumptions were used. For instance, in [31] it was assumed that $c_w^2 C_{WW} = s_w^2 C_{BB}$ that means $g_{a\gamma Z} = 0$, $g_{a\gamma Z} = g_{aZZ}$. It was obtained that the sensitivity bound on $g_{a\gamma Z}$ for the third stage for the CLIC in the ALP mass interval 5 GeV—2600 GeV is equal to 0.091 TeV^{-1} at 5σ level [106]. It is compatible with our bound for the 3 TeV muon collider in the region $m_a = 10$–1000 GeV, see figure 5. For the interval $m_a = 1000$–3000 GeV our bound is significantly stronger. In general, C_{WW} and C_{BB} are independent parameters, so are the couplings $g_{a\gamma Z}$ and g_{aZZ}. In particular, for the FCC-ee and LHC-allowed regions in the parameter space $g_{a\gamma Z} - g_{aZZ}$ have been obtained in [23]. Note that the 95% CL upper limit on $g_{a\gamma\gamma}$ extracted from CMS Run 2 measurements is equal to 4.99 TeV^{-1}, while for the HL-LHC the projected limit is 2.43 TeV^{-1} [19].

3. Unitarity constraints on ALP coupling

Let us study bounds imposed by partial-wave unitarity. The partial-wave expansion of the helicity amplitude in the center-of-mass system was derived in [106]. It looks like

$$M_{\lambda_1\lambda_2\lambda_3\lambda_4}(s,\,\theta,\,\varphi) = 16\pi\sum_J (2J+1)\sqrt{(1+\delta_{\lambda_1\lambda_2})(1+\delta_{\lambda_3\lambda_4})} \times e^{i(\lambda-\mu)\phi}\, d^J_{\lambda\mu}(\theta)\, T^J_{\lambda_1\lambda_2\lambda_3\lambda_4}(s), \tag{17}$$

where $\lambda = \lambda_1 - \lambda_2$, $\mu = \lambda_3 - \lambda_4$, $\theta(\phi)$ is the polar (azimuth) scattering angle, and $d^J_{\lambda\mu}(\theta)$ is the Wigner (small) d-function [107]. Relevant formulas for the d-functions can be found in [108]. If we choose the plane $(x - z)$ as a scattering plane, then $\phi = 0$ in (17). Parity conservation means that

$$T^J_{\lambda_1\lambda_2\lambda_3\lambda_4}(s) = (-1)^{\lambda_1-\lambda_2-\lambda_3+\lambda_4}\, T^J_{-\lambda_1-\lambda_2-\lambda_3-\lambda_4}(s). \tag{18}$$

Partial-wave unitarity in the limit $s \gg (m_1 + m_2)^2$ requires that

$$|T^J_{\lambda_1\lambda_2\lambda_3\lambda_4}(s)| \leqslant 1. \tag{19}$$

Using orthogonality of the d-functions,

$$\int_{-1}^{1} \mathrm{d}^J_{\lambda\lambda'}(z)\, d^{J'}_{\lambda\lambda'}(z)\, \mathrm{d}z = \frac{2}{2J+1}\,\delta_{JJ'}, \tag{20}$$

we find from (17) that the partial-wave amplitude is defined as

$$T^J_{\lambda_1\lambda_2\lambda_3\lambda_4}(s) = \frac{1}{32\pi}\frac{1}{\sqrt{(1+\delta_{\lambda_1\lambda_2})(1+\delta_{\lambda_3\lambda_4})}}\int_{-1}^{1} M_{\lambda_1\lambda_2\lambda_3\lambda_4}(s,\,z)\,\mathrm{d}^J_{\lambda\mu}(z)\,\mathrm{d}z. \tag{21}$$

Here and in what follows, $z = \cos\theta$. The helicity amplitudes $M_{\lambda_1\lambda_2\lambda_3\lambda_4}$ are given in appendix.

The d-functions obey, inter alia, the relation $d^J_{\lambda\mu}(-z) = (-1)^{J-\lambda} d^J_{\mu-\lambda}(z)$. In particular, we have $(J \geqslant 0)$

$$d^J_{00}(z) = P_J(z), \tag{22}$$

$P_J(z)$ being the Legendre polynomial, and [108]

$$d^J_{2-2}(z) = (-1)^J\left(\frac{1-z}{2}\right)^2 {}_2F_1\!\left(2-J,\,J+3;\,1;\,\frac{1+z}{2}\right), \tag{23}$$

$$d^J_{22}(z) = \left(\frac{1+z}{2}\right)^2 {}_2F_1\!\left(2-J,\,J+3;\,1;\,\frac{1-z}{2}\right), \tag{24}$$

where ${}_2F_1(a, b; c; x)$ is the hypergeometric function [109], and $J \geqslant 2$.

1. Consider the helicity amplitude $M^{\gamma\gamma}_{++++}$ (A3). Then $\lambda_1 = \lambda_2 = \lambda_3 = \lambda_4 = 1$, and $\lambda = \mu = 0$. Since s, $m_a^2 \gg m_a\Gamma_a$, we can write

$$M_{++++}^{\gamma\gamma}(s, z) = -\frac{4}{f_a^2}\frac{s^2}{s - m_a^2}. \tag{25}$$

The partial-wave amplitude with $J = 0$ is the only non-zero amplitude, since

$$T_{++++}^J(s) = -\frac{1}{16\pi f_a^2}\frac{s^2}{s - m_a^2}\int_{-1}^{1} P_J(z)\,\mathrm{d}z = -\frac{1}{8\pi f_a^2}\frac{s^2}{s - m_a^2}\delta_{J0}. \tag{26}$$

Then we obtain from (19), (26) the unitarity bound on the the ALP-gauge boson coupling coupling

$$f_a^2 \geqslant \frac{1}{8\pi}\frac{s}{|1 - \varepsilon|}, \tag{27}$$

where $\varepsilon = m_a^2/s$.

2. For the helicity amplitude $M_{++--}^{\gamma\gamma}$ (A7) we have $\lambda_1 = \lambda_2 = 1$, $\lambda_3 = \lambda_4 = -1$, and, consequently, $\lambda = 0$, $\mu = 0$. It looks like (A7)

$$M_{++--}^{\gamma\gamma}(s, z) = \frac{2s}{f_a^2}\left[\frac{2}{1 - \varepsilon} - \frac{(1 - z)^2}{1 - z + 2\varepsilon} - \frac{(1 + z)^2}{1 + z + 2\varepsilon}\right]. \tag{28}$$

As a result, we obtain

$$\begin{aligned} T_{++--}^J(s) &= \frac{s}{32\pi f_a^2}\left[\frac{2}{1 - \varepsilon}\int_{-1}^{1} P_J(z)\,\mathrm{d}z - (1 + (-1)^J)\int_{-1}^{1}\frac{(1 - z)^2}{1 - z + 2\varepsilon}P_J(z)\,\mathrm{d}z\right] \\ &= \frac{s}{8\pi f_a^2}\left[\frac{\varepsilon(3 - 2\varepsilon)}{1 - \varepsilon}\delta_{J0} - (1 + (-1)^J)\varepsilon^2 Q_J(1 + 2\varepsilon)\right], \end{aligned} \tag{29}$$

where $Q_J(x)$ is the Legendre function of the second kind [110]. If $x > 1$, $Q_J(x)$ is a real strictly decreasing function of J, and it decreases exponentially as $J \to \infty$. Note that $Q_J(1 + 2\varepsilon) \simeq -(\ln\varepsilon)/2$ for $\varepsilon \ll 1$, $J \geqslant 0$. The term with $J = 0$ is a leading one,

$$T_{++--}^0(s) = \frac{s}{8\pi f_a^2}\,\varepsilon\left[\frac{3 - 2\varepsilon}{1 - \varepsilon} - \varepsilon\ln\frac{1 + \varepsilon}{\varepsilon}\right]. \tag{30}$$

It results in the following unitarity bound

$$f_a^2 \geqslant \frac{s}{8\pi}\,\varepsilon\left|\frac{3 - 2\varepsilon}{1 - \varepsilon} - \varepsilon\ln\frac{1 + \varepsilon}{\varepsilon}\right|. \tag{31}$$

3. Now consider the helicity amplitude $M_{+--+}^{\gamma\gamma}$ (A8). Then $\lambda_1 = \lambda_4 = 1$, $\lambda_2 = \lambda_3 = -1$, and $\lambda = 2$, $\mu = -2$. The helicity amplitude is given by equation (A8)

$$M_{+--+}^{\gamma\gamma}(s, z) = \frac{2}{f_a^2}\frac{s(1 - z)^2}{1 - z + 2\varepsilon}. \tag{32}$$

Then we get from (21), (23), (32)

$$\begin{aligned} T_{+--+}^J(s) &= (-1)^J\frac{s}{64\pi f_a^2}\int_{-1}^{1}\frac{(1 - z)^4}{1 - z + 2\varepsilon}\,{}_2F_1\!\left(2 - J, J + 3; 1; \frac{1 + z}{2}\right)\mathrm{d}z \\ &= (-1)^J\frac{s}{4\pi f_a^2}I(J, \varepsilon), \end{aligned} \tag{33}$$

where the notation

$$I(J, \varepsilon) = \int_0^1 \frac{x^4}{x + \varepsilon}\,{}_2F_1(2 - J, J + 3; 1; 1 - x)\,\mathrm{d}x \tag{34}$$

is introduced. Using formula 2.21.1.26 in [111], we obtain a sequence of two equalities (recall that $J \geqslant 2$)

$$I(J,\, \varepsilon) = \frac{\Gamma(5)}{\varepsilon\, \Gamma(3 - J)\Gamma(J + 4)}\, {}_3F_2\left(1;\, 1;\, 5;\, 3 - J;\, J + 4;\, -\frac{1}{\varepsilon}\right)$$
$$= (-1)^J\, \frac{\Gamma(J - 1)\Gamma(J + 3)}{\varepsilon^{J-1}\, \Gamma(2J + 2)}\, {}_2F_1\left(J - 1,\, J + 3;\, 2J + 2;\, -\frac{1}{\varepsilon}\right), \tag{35}$$

where $\Gamma(x)$ denotes the gamma function [109]. In (35) we have reduced a generalized hypergeometric function ${}_3F_2(a, b, c; d, e; x)$ to a traditional hypergeometric function. With the help of equation (2).10(6) in [109] we find the final analytic expression for $I(J, \varepsilon)$,

$$I(J,\, \varepsilon) = (-1)^J (1 + \varepsilon)^{1-J}\, \frac{\Gamma(J - 1)\Gamma(J + 3)}{\Gamma(2J + 2)}$$
$$\times\, {}_2F_1\left(J - 1,\, J - 1;\, 2J + 2;\, \frac{1}{1 + \varepsilon}\right). \tag{36}$$

Using integral representation for the hypergeometric function (see formula 2.12(1) in [109]), one can show that for $\varepsilon > 0$ the right-hand side of equation (36) is a strictly decreasing function of J. Moreover, it falls off exponentially at large J. Thus, the most stringent unitarity bound comes from the partial-wave amplitude with $J = 2$ that looks like

$$T^2_{+--+}(s) = \frac{s}{20\pi f_a^2} \frac{1}{1 + \varepsilon}\, {}_2F_1\left(1,\, 1;\, 6;\, \frac{1}{1 + \varepsilon}\right)$$
$$= \frac{s}{16\pi f_a^2}\left[1 - \frac{4\varepsilon}{3} + 2\varepsilon^2 - 4\varepsilon^3 + 4\varepsilon^4 \ln\frac{1 + \varepsilon}{\varepsilon}\right]. \tag{37}$$

As a result, we come to the unitarity bound

$$f_a^2 \geqslant \frac{s}{16\pi}\left|1 - \frac{4\varepsilon}{3} + 2\varepsilon^2 - 4\varepsilon^3 + 4\varepsilon^4 \ln\frac{1 + \varepsilon}{\varepsilon}\right|. \tag{38}$$

Note that the right-hand side of this equation does not exceed $s/(16\pi)$.

The analogous examination of the amplitude $M^{\gamma\gamma}_{+-+-}$, using equations (A9) and (24), results in just the same bound (38).

The unitarity constraints for the amplitudes $M^{Z\gamma}_{\lambda_1\lambda_2\lambda_3\lambda_4}$ and $M^{ZZ}_{\lambda_1\lambda_2\lambda_3\lambda_4}$ differ from the above presented bounds for $M^{\gamma\gamma}_{\lambda_1\lambda_2\lambda_3\lambda_4}$ (with the same helicities) by the factors $2s_w/c_w \simeq 1.1$ and $s_w^2/c_w^2 \simeq 0.3$, respectively, neglecting small corrections of $\mathrm{O}(m_Z/\sqrt{s})$ or $\mathrm{O}(m_Z^2/s)$. In particular, imposing unitarity constraint on the amplitude $M^{Z\gamma}_{++++}$, we get the lower bound (up to small corrections $\mathrm{O}(m_Z^2/s)$)

$$f_a^2 \geqslant \frac{1}{4\pi} \frac{s_w}{c_w} \frac{s}{|1 - \varepsilon|}. \tag{39}$$

This constraint is slightly stronger than (27). Unitarity bounds for most of the other helicity amplitudes with the Z boson(s) are suppressed by small factors $m_Z/\sqrt{s}$ or m_Z^2/s. The constraint (39) appears to be the strongest unitary bound.

The bound (39) has been derived by neglecting ALP width Γ_2 (5) which, in its turn, depends on f_a, see equation (6). If we will take the ALP width into account, our bound (39) is modified as follows,

$$\frac{s_w}{c_w}\frac{s^2}{\sqrt{16\pi^2 f_a^4 (s - m_a^2)^2 + m_a^8/[\mathrm{Br}(a \to \gamma\gamma)]^2}} \leqslant 1. \tag{40}$$

We see that in the large mass region $m_a^2 \geqslant s\sqrt{(s_w/c_w)\mathrm{Br}(a \to \gamma\gamma)}$ inequality (40) is satisfied for *all* f_a. It means that for such values of m_a there is no unitary limit. In the region $m_a^2 < s\sqrt{(s_w/c_w)\mathrm{Br}(a \to \gamma\gamma)}$ we obtain from (40) that the following inequality takes place

$$f_a^2 > \frac{s\sqrt{(s_w/c_w)^2 - \varepsilon^4/[\mathrm{Br}(a \to \gamma\gamma)]^2}}{4\pi(1 - \varepsilon)}. \tag{41}$$

In the limit $\Gamma_a \to 0$ (which is equivalent to the limit $\mathrm{Br}(a \to \gamma\gamma) \to \infty$), we reproduce equation (39). The unitary bounds for different center-of-mass energies and ALP branching ratios are presented in figure 5. We conclude that the unitarity is not violated in the region of the ALP coupling f_a^{-1} studied in the present paper.

4. Conclusions

The different ALP production mechanisms at high-energy muon collider offer a rich phenomenology, allowing us to examine a large range of the ALP mass and couplings. In the present paper, we have examined the possibility to search for heavy axion-like particles in the $\mu^+\mu^- \to \mu^+\gamma\gamma\mu^-$ scattering at the future muon collider. The studies are presented for the collision energies of 3 TeV, 14 TeV, and 100 TeV and integrated luminosities of 1 ab^{-1}, 20 ab^{-1}, and 1000 ab^{-1}, respectively. We have obtained the explicit expressions for the helicity amplitudes for the $Z\gamma \to \gamma\gamma$ and $ZZ \to \gamma\gamma$ collisions. Using these amplitudes (as well as known helicity amplitudes for the $\gamma\gamma \to \gamma\gamma$ collision), the differential cross sections versus invariant mass of the final photons and total cross section versus minimal diphoton invariant mass are calculated. As a result, the 95% C.L. exclusion regions for the ALP-gauge boson coupling coming from the $\mu^+\mu^- \to \mu^+\gamma\gamma\mu^-$ scattering at the high-energy muon collider are obtained. The excluded areas extend to wider regions in comparison to the region obtained previously for the polarized light-by-light scattering at the 3 TeV CLIC. Our constraints are also much stronger than the current experimental bounds presented in figure 6. The partial-wave unitarity bounds on the ALP-gauge boson coupling are estimated. We have shown that the unitarity is not violated in the region of the ALP coupling which has been studied in our paper. We can conclude that the future muon collider has a great physical potential in searching for axion-like particle couplings to the SM gauge bosons.

Data availability statement

No new data were created or analyzed in this study.

Appendix. Helicity amplitudes

A.1. $\gamma\gamma \to \gamma\gamma$ scattering

The Mandelstam variables for the $\gamma\gamma \to \gamma\gamma$ collision satisfy the relation $s + t + u = 0$, and we get

$$\cos\theta = \frac{u - t}{u + t}, \quad \sin\theta = -\frac{2\sqrt{tu}}{t + u}, \tag{A1}$$

$$t = -\frac{s}{2}(1 - \cos\theta), \quad u = -\frac{s}{2}(1 + \cos\theta). \tag{A2}$$

The helicity amplitudes of the LBL scattering are known to be [12]

$$M^{\gamma\gamma}_{++++} = -\frac{4}{f_a^2}\frac{s^2}{s - m_a^2 + im_a\Gamma_a}, \tag{A3}$$

$$M^{\gamma\gamma}_{+++-} = 0, \tag{A4}$$

$$M^{\gamma\gamma}_{++-+} = 0, \tag{A5}$$

$$M^{\gamma\gamma}_{+-++}0, \tag{A6}$$

$$M^{\gamma\gamma}_{++--} = \frac{4}{f_a^2}\frac{s^2}{s - m_a^2 + im_a\Gamma_a} + \frac{s^2}{f_a^2}\left[\frac{(1 - \cos\theta)^2}{t - m_a^2 + im_a\Gamma_a} + \frac{(1 + \cos\theta)^2}{u - m_a^2 + im_a\Gamma_a}\right], \tag{A7}$$

$$M^{\gamma\gamma}_{+--+} = -\frac{1}{f_a^2}\frac{s^2(1 - \cos\theta)^2}{t - m_a^2 + im_a\Gamma_a}, \tag{A8}$$

$$M^{\gamma\gamma}_{+-+-} = -\frac{1}{f_a^2}\frac{s^2(1 + \cos\theta)^2}{u - m_a^2 + im_a\Gamma_a}, \tag{A9}$$

$$M^{\gamma\gamma}_{+---} = 0. \tag{A10}$$

Other helicity amplitudes $M^{\gamma\gamma}_{\lambda_1\lambda_2\lambda_3\lambda_4}$ can be obtained by the P-parity relation

$$M^{\gamma\gamma}_{\lambda_1\lambda_2\lambda_3\lambda_4} = M^{\gamma\gamma}_{-\lambda_1-\lambda_2-\lambda_3-\lambda_4}. \tag{A11}$$

A.2. $Z\gamma \to \gamma\gamma$ scattering

The Mandelstam variables for this process obey the relation $s + t + u = m_Z^2$, variables $\cos\theta$, $\sin\theta$ are given by equation (A1), and

$$t = -\frac{s - m_Z^2}{2}(1 - \cos\theta), \quad u = -\frac{s - m_Z^2}{2}(1 + \cos\theta). \tag{A12}$$

Our calculations result in the following analytic expressions for the helicity amplitudes of the $Z\gamma \to \gamma\gamma$ process:

$$M^{Z\gamma}_{++++} = \frac{8s_w}{c_w}\frac{1}{f_a^2}\frac{s(s - m_Z^2)}{s - m_a^2 + im_a\Gamma_a}, \tag{A13}$$

$$M^{Z\gamma}_{+++-} = \frac{2s_w}{c_w}\frac{1}{f_a^2}\frac{m_Z^2(s - m_Z^2)(\sin\theta)^2}{t - m_a^2 + im_a\Gamma_a}, \tag{A14}$$

$$M^{Z\gamma}_{++-+} = \frac{2s_w}{c_w}\frac{1}{f_a^2}\frac{m_Z^2(s - m_Z^2)(\sin\theta)^2}{u - m_a^2 + im_a\Gamma_a}, \tag{A15}$$

$$M^{Z\gamma}_{+-++} = -\frac{2s_w}{c_w}\frac{1}{f_a^2}\, m_Z^2(s - m_Z^2)(\sin\theta)^2 \times \left[\frac{1}{t - m_a^2 + im_a\Gamma_a} + \frac{1}{u - m_a^2 + im_a\Gamma_a}\right], \tag{A16}$$

$$M^{Z\gamma}_{++--} = -\frac{8s_w}{c_w}\frac{1}{f_a^2}\frac{s(s - m_Z^2)}{s - m_a^2 + im_a\Gamma_a} - \frac{2s_w}{c_w}\frac{1}{f_a^2}\, s(s - m_Z^2) \times \left[\frac{(1 - \cos\theta)^2}{t - m_a^2 + im_a\Gamma_a} + \frac{(1 + \cos\theta)^2}{u - m_a^2 + im_a\Gamma_a}\right], \tag{A17}$$

$$M^{Z\gamma}_{+--+} = \frac{2s_w}{c_w}\frac{1}{f_a^2}\frac{s(s - m_Z^2)(1 - \cos\theta)^2}{t - m_a^2 + im_a\Gamma_a}, \tag{A18}$$

$$M^{Z\gamma}_{+-+-} = \frac{2s_w}{c_w}\frac{1}{f_a^2}\frac{s(s - m_Z^2)(1 + \cos\theta)^2}{u - m_a^2 + im_a\Gamma_a}, \tag{A19}$$

$$M^{Z\gamma}_{+---} = 0, \tag{A20}$$

$$M^{Z\gamma}_{0+++} = 0, \tag{A21}$$

$$M^{Z\gamma}_{0++-} = \frac{4i}{\sqrt{2}}\frac{s_w}{c_w}\frac{1}{f_a^2}\frac{m_Z\sqrt{s}(s - m_Z^2)(1 - \cos\theta)\sin\theta}{t - m_a^2 + im_a\Gamma_a}, \tag{A22}$$

$$M^{Z\gamma}_{0+-+} = -\frac{4i}{\sqrt{2}}\frac{s_w}{c_w}\frac{1}{f_a^2}\frac{m_Z\sqrt{s}(s - m_Z^2)(1 + \cos\theta)\sin\theta}{u - m_a^2 + im_a\Gamma_a}, \tag{A23}$$

$$M^{Z\gamma}_{0-++} = \frac{4i}{\sqrt{2}}\frac{s_w}{c_w}\frac{1}{f_a^2}\, m_Z\sqrt{s}(s - m_Z^2)\sin\theta \times \left[\frac{(1 - \cos\theta)}{t - m_a^2 + im_a\Gamma_a} - \frac{(1 + \cos\theta)}{u - m_a^2 + im_a\Gamma_a}\right], \tag{A24}$$

$$M^{Z\gamma}_{0+--} = -\frac{4i}{\sqrt{2}}\frac{s_w}{c_w}\frac{1}{f_a^2}\, m_Z\sqrt{s}(s - m_Z^2)\sin\theta \times \left[\frac{(1 - \cos\theta)}{t - m_a^2 + im_a\Gamma_a} - \frac{(1 + \cos\theta)}{u - m_a^2 + im_a\Gamma_a}\right], \tag{A25}$$

$$M^{Z\gamma}_{0--+} = \frac{4i}{\sqrt{2}}\frac{s_w}{c_w}\frac{1}{f_a^2}\frac{m_Z\sqrt{s}(s - m_Z^2)(1 - \cos\theta)\sin\theta}{t - m_a^2 + im_a\Gamma_a}. \tag{A26}$$

Other amplitudes $M^{Z\gamma}_{\lambda_1\lambda_2\lambda_3\lambda_4}$ can be obtained by relation [84]

$$M^{Z\gamma}_{\lambda_1\lambda_2\lambda_3\lambda_4} = (-1)^{1-\lambda_1} M^{Z\gamma}_{-\lambda_1-\lambda_2-\lambda_3-\lambda_4}, \tag{A27}$$

where λ_1 is a helicity of the Z boson.

A.3. $ZZ \to \gamma\gamma$ scattering

The Mandelstam variables obey the relation $s + t + u = 2m_Z^2$, and we obtain

$$\cos\theta = \frac{t - u}{\sqrt{(t + u)^2 - 4m_Z^4}}, \quad \sin\theta = \frac{2\sqrt{tu - m_Z^4}}{\sqrt{(t + u)^2 - 4m_Z^4}}, \tag{A28}$$

$$\begin{aligned} t &= -\frac{1}{2}[(s - 2m_Z^2) - \sqrt{s(s - 4m_Z^2)}\cos\theta], \\ u &= -\frac{1}{2}[(s - 2m_Z^2) + \sqrt{s(s - 4m_Z^2)}\cos\theta]. \end{aligned} \tag{A29}$$

We have derived the following helicity amplitudes of the $ZZ \to \gamma\gamma$ process:

$$\begin{aligned} M_{++++}^{ZZ} = &-\frac{4s_w^2}{c_w^2}\frac{1}{f_a^2}\frac{s^{3/2}\sqrt{s - 4m_Z^2}}{s - m_a^2 + im_a\Gamma_a} + \frac{s_w^2}{c_w^2}\frac{1}{f_a^2}s(\sqrt{s} - \sqrt{s - 4m_Z^2})^2 \\ &\times \left[\frac{(1 + \cos\theta)^2}{t - m_a^2 + im_a\Gamma_a} + \frac{(1 - \cos\theta)^2}{u - m_a^2 + im_a\Gamma_a}\right], \end{aligned} \tag{A30}$$

$$\begin{aligned} M_{+++-}^{ZZ} = &-\frac{4s_w^2}{c_w^2}\frac{1}{f_a^2}m_Z^2 s(\sin\theta)^2 \\ &\times \left[\frac{1}{t - m_a^2 + im_a\Gamma_a} + \frac{1}{u - m_a^2 + im_a\Gamma_a}\right], \end{aligned} \tag{A31}$$

$$\begin{aligned} M_{+-++}^{ZZ} = &\frac{4s_w^2}{c_w^2}\frac{1}{f_a^2}m_Z^2 s(\sin\theta)^2 \\ &\times \left[\frac{1}{t - m_a^2 + im_a\Gamma_a} + \frac{1}{u - m_a^2 + im_a\Gamma_a}\right], \end{aligned} \tag{A32}$$

$$\begin{aligned} M_{+-+-}^{ZZ} = &-\frac{s_w^2}{c_w^2}\frac{1}{f_a^2}(1 + \cos\theta)^2 \\ &\times \left\{\frac{[s - \sqrt{s(s - 4m_Z^2)}]^2}{t - m_a^2 + im_a\Gamma_a} + \frac{[s + \sqrt{s(s - 4m_Z^2)}]^2}{u - m_a^2 + im_a\Gamma_a}\right\}, \end{aligned} \tag{A33}$$

$$\begin{aligned} M_{++--}^{ZZ} = &\frac{4s_w^2}{c_w^2}\frac{1}{f_a^2}\frac{s^{3/2}\sqrt{s - 4m_Z^2}}{s - m_a^2 + im_a\Gamma_a} + \frac{s_w^2}{c_w^2}\frac{1}{f_a^2}[s + \sqrt{s(s - 4m_Z^2)}]^2 \\ &\times \left[\frac{(1 - \cos\theta)^2}{t - m_a^2 + im_a\Gamma_a} + \frac{(1 + \cos\theta)^2}{u - m_a^2 + im_a\Gamma_a}\right], \end{aligned} \tag{A34}$$

$$M^{ZZ}_{+--+} = -\frac{s_w^2}{c_w^2}\frac{1}{f_a^2}(1 - \cos\theta)^2 \times \left\{\frac{[s + \sqrt{s(s - 4m_Z^2)}\,]^2}{t - m_a^2 + im_a\Gamma_a} + \frac{[s - \sqrt{s(s - 4m_Z^2)}\,]^2}{u - m_a^2 + im_a\Gamma_a}\right\}, \tag{A35}$$

$$M^{ZZ}_{0+++} = \frac{4i}{\sqrt{2}}\frac{s_w^2}{c_w^2}\frac{1}{f_a^2}\, m_Z s(\sqrt{s} - \sqrt{s - 4m_Z^2})\sin\theta \times \left[\frac{(1 + \cos\theta)}{t - m_a^2 + im_a\Gamma_a} - \frac{(1 - \cos\theta)}{u - m_a^2 + im_a\Gamma_a}\right], \tag{A36}$$

$$M^{ZZ}_{0++-} = -\frac{4i}{\sqrt{2}}\frac{s_w^2}{c_w^2}\frac{1}{f_a^2}\, m_Z\sqrt{s}\,(1 - \cos\theta)\sin\theta \times \left[\frac{s + \sqrt{s(s - 4m_Z^2)}}{t - m_a^2 + im_a\Gamma_a} + \frac{s - \sqrt{s(s - 4m_Z^2)}}{u - m_a^2 + im_a\Gamma_a}\right], \tag{A37}$$

$$M^{ZZ}_{0-++} = \frac{4i}{\sqrt{2}}\frac{s_w^2}{c_w^2}\frac{1}{f_a^2}\, m_Z\sqrt{s}\,[s + \sqrt{s(s - 4m_Z^2)}\,]\sin\theta \times \left[\frac{1 - \cos\theta}{t - m_a^2 + im_a\Gamma_a} - \frac{1 + \cos\theta}{u - m_a^2 + im_a\Gamma_a}\right], \tag{A38}$$

$$M^{ZZ}_{0+-+} = \frac{4i}{\sqrt{2}}\frac{s_w^2}{c_w^2}\frac{1}{f_a^2}\, m_Z\sqrt{s}\,(1 + \cos\theta)\sin\theta \times \left[\frac{s - \sqrt{s(s - 4m_Z^2)}}{t - m_a^2 + im_a\Gamma_a} + \frac{s + \sqrt{s(s - 4m_Z^2)}}{u - m_a^2 + im_a\Gamma_a}\right], \tag{A39}$$

$$M^{ZZ}_{0+--} = -\frac{4i}{\sqrt{2}}\frac{s_w^2}{c_w^2}\frac{1}{f_a^2}\, m_Z\sqrt{s}\,[s + \sqrt{s(s - 4m_Z^2)}\,]\sin\theta \times \left[\frac{1 - \cos\theta}{t - m_a^2 + im_a\Gamma_a} - \frac{1 + \cos\theta}{u - m_a^2 + im_a\Gamma_a}\right], \tag{A40}$$

$$M^{ZZ}_{00++} = -\frac{8s_w^2}{c_w^2}\frac{1}{f_a^2}\, m_Z^2 s(\sin\theta)^2 \times \left[\frac{1}{t - m_a^2 + im_a\Gamma_a} + \frac{1}{u - m_a^2 + im_a\Gamma_a}\right], \tag{A41}$$

$$M_{00+-}^{ZZ} = -\frac{8s_w^2}{c_w^2}\frac{1}{f_a^2}\, m_Z^2 s (\sin\theta)^2 \times \left[\frac{1}{t - m_a^2 + i m_a \Gamma_a} + \frac{1}{u - m_a^2 + i m_a \Gamma_a}\right]. \qquad \text{(A42)}$$

Other helicity amplitudes $M_{\lambda_1\lambda_2\lambda_3\lambda_4}^{ZZ}$ can be obtained using relation [85]

$$M_{\lambda_1\lambda_2\lambda_3\lambda_4}^{ZZ} = (-1)^{\lambda_1-\lambda_2} M_{-\lambda_1-\lambda_2-\lambda_3-\lambda_4}^{ZZ}, \qquad \text{(A43)}$$

where λ_1, λ_2 are helicities of the colliding Z bosons.

ORCID iDs

A V Kisselev https://orcid.org/0000-0003-4362-9952

References

[1] Peccei R D and Quinn H R 1977 CP conservation in the presence of pseudoparticles *Phys. Rev. Lett.* **38** 1440
[2] Peccei R D and Quinn H R 1977 Constraints imposed by CP conservation in the presence of pseudoparticles *Phys. Rev.* D **16** 1791
[3] Weinberg S 1978 A new light boson? *Phys. Rev. Lett.* **40** 223
[4] Wilzcek F 1978 Problem of strong P and T invariance in the presence of instantons *Phys. Rev. Lett.* **40** 279
[5] Preskill J, Wise M B and Wilczek F 1983 Cosmology of the invisible axion *Phys. Lett.* B **120** 127
[6] Abbott L F and Sikivie P 1983 A cosmological bound on the invisible axion *Phys. Lett.* B **120** 133
[7] Dine M and Fischler W 1983 The not so harmless axion *Phys. Lett.* B **120** 137
[8] Chadha-Day F, Ellis J and Marsh D J E Axion dark matter: what is it and why now? arXiv:2105.01406
[9] Marsh D J E 2016 Axion cosmology *Phys. Rep.* **643** 1
[10] Abbott L F and Sikivie P 1983 A cosmological bound on the invisible axion *Phys. Lett.* B **120** 133
[11] Sikivie P 2008 Axion cosmology *Lect. Notes Phys.* **741** 19
[12] Baldenegro C, Fichet S, von Gersdorff G and Royon C 2018 Searching for axion-like particles with proton tagging at the LHC *J. High Energy Phys.* JHEP06(2018)131
[13] Baldenegro C, Hassani S, Royon C and Schoeffel L 2019 Extending the constraint for axion-like particles as resonances at the LHC and laser beam experiments *Phys. Lett.* B **795** 339
[14] Carra S *et al* 2021 Constraining off-shell production of axion-like particles with $Z\gamma$ and WW differential cross-section measurements *Phys. Rev.* D **104** 092005
[15] Ren J, Wang D, Wu L, Yang J M and Zhang M 2021 Detecting an axion-like particle with machine learning at the LHC *J. High Energy Phys.* JHEP11(2021)138
[16] Flórez A *et al* 2021 Probing axion-like particles with $\gamma\gamma$ final states from vector boson fusion processes at the LHC *Phys. Rev.* D **103** 095001
[17] Wang D, Wu L, Yang J M and Zhang M 2021 Photon-jet events as a probe of axion-like particles at the LHC *Phys. Rev.* D **104** 095016
[18] d'Enterria D Collider constraints on axion-like particles, in workshop on feebly interacting particles arXiv:2102.08971
[19] Bonilla J, Brivio I, Machado-Rodriguez J and de Troconiz J F 2022 Nonresonant searches for axion-like particles in vector boson scattering processes at the LHC *J. High Energy Phys.* JHEP06(2022)113
[20] Bauer M, Neubert M and Thamm A 2017 Collider probes of axion-like particles *J. High Energy Phys.* JHEP12(2017)044
[21] Knapen S, Lin T, Lou H K and Melia T 2017 Searching for axion-like particles with ultra-peripheral heavy-ion collisions *Phys. Rev. Lett.* **118** 171801

[22] Knapen S, Lin T, Lou H K and Melia T 2018 LHC limits on axion-like particles from heavy-ion collisions *Proc. of the PHOTON 2017 Conf. (Geneva, Switzerland, 22–26 May, 2017)* ed D d'Enterria *et al* vol 1 pp 65–8
[23] Bauer M, Heiles M, Neubert M and Thamm A 2019 Axion-like particles at future colliders *Eur. Phys. J.* C **79** 74
[24] İnan S C and Kisselev A V 2020 A search for axion-like particles in light-by-light scattering at the CLIC *J. High Energy Phys.* JHEP06(2020)183
[25] İnan S C and Kisselev A V 2021 Polarized light-by-light scattering at the CLIC induced by axion-like particles *Chin. Phys.* C **45** 043109
[26] Steinberg N Discovering axion-like particles with photon fusion at the ILC arXiv:2108.11927
[27] Zhang H-Y, Yue C-X, Guo Y-C and Yang S 2021 Searching for axionlike particles at future electron- positron colliders *Phys. Rev.* D **104** 096008
[28] Agrawal P *et al* 2021 Feebly-interacting particles: FIPs 2020 workshop report *Eur. Phys. J.* C **81** 1015
[29] Tian M, Wang K and Wan Z S Search for long-lived axions with far detectors at future lepton colliders arXiv:2201.08960
[30] Schäfer R, Tillinger F and Westhoff S Near or far detectors? Optimizing long-lived particle searches at electron-positron colliders arXiv:2202.11714
[31] Yue C-X, Zhang H-Y and Wang H 2022 Production of axion-like particles via vector boson fusion at future electron-positron colliders *Eur. Phys. J.* C **82** 88
[32] Liu Y and Yan B Searching for the axion-like particle at the EIC arXiv:2112.02477
[33] Davoudiasl H, Marcarelli R and Neil E T Lepton-flavor-violating ALPs at the electron-ion collider: a golden opportunity arXiv:2112.04513
[34] Kim J E 1987 Light pseudoscalars, particle physics and cosmology *Phys. Rep.* **150** 1
[35] Peccei R D 2008 The Strong CP problem and axions *Lect. Notes Phys.* **741** 3
[36] Raffelt G G 2008 Astrophysical axion bounds *Lect. Notes Phys.* **741** 51
[37] Marsh D J E Axions and ALPs: a very short introduction arXiv:1712.03018
[38] Irastorza I G and Redondo J 2018 New experimental approaches in the search for axion-like particles *Prog. Part. Nucl. Phys.* **102** 89
[39] Irastorza I G 2022 An introduction to axions and their detection *SciPost Phys. Lect. Notes* **45** 1
[40] Aaboud M *et al* (ATLAS Collaboration) 2017 Evidence for light-by-light scattering in heavy-ion collisions with the ATLAS detector at the LHC *Nat. Phys.* **13** 852
[41] Aad G *et al* (ATLAS Collaboration) 2019 Observation of light-by-light scattering in ultraperipheral Pb+Pb collisions with the ATLAS detector *Phys. Rev. Lett.* **123** 052001
[42] d'Enterria D *et al* (CMS Collaboration) 2019 Evidence for light-by-light scattering in ultraperipheral PbPb collisions at $\sqrt{s} = 5.02$ TeV *Nucl. Phys.* A **982** 791
[43] d'Enterria D and da Silveira G G 2013 Observing light-by-light scattering at the large hadron collider *Phys. Rev. Lett.* **111** 080405
[44] Coelho R O, Goncalves V P, Martins D E and Rangel M S 2020 Exclusive and diffraction $\gamma\gamma$ production in *PbPb* collisions at the LHC, HE-LHC and FCC *Eur. Phys. J.* C **80** 488
[45] Coelho R O, Goncalves V P, Martins D E and Rangel M S 2020 Production of axionlike particles in *PbPb* collisions at the LHC, HE-LHC and FCC: a phenomenological analysis *Phys. Lett.* **806** 135512
[46] Atağ S, İnan S C and Şahin İ 2010 Extra dimensions in $\gamma\gamma \to \gamma\gamma$ process at the CERN-LHC *J. High Energy Phys.* JHEP09(2010)042
[47] İnan S C and Kisselev A V 2019 Probe of the Randall-Sundrum-like model with the small curvature via light-by-light scattering at the LHC *Phys. Rev.* D **100** 095004
[48] İnan S C and Kisselev A V 2021 quartic $\gamma\gamma\gamma\gamma$ couplings in light-by-light collisions at the CLIC *Eur. Phys. J.* C **81** 664
[49] Ellis J, Mavromatos N E, Roloff P and You T Light-by-light scattering at future e^+e^- colliders arXiv:2203.17111
[50] Haghighat G and Najafabadi M M Search for lepton-flavor-violating ALPs at a future muon collider and utilization of polarization-induced effects arXiv:2106.00505
[51] Casarsa M, Fabbrichesi M and Gabrielli E 2022 Mono-chromatic single photon events at the muon collider *Phys. Rev.* D **105** 075008
[52] Bao Y, Fan J J and Li L Electroweak ALP searches at a muon collider arXiv:2203.04328
[53] Han T, Li T and Wang X 2021 Axion-like particles at high energy muon colliders—a white paper for snowmass arXiv:2203.05484

[54] Tikhonin F F 1968 On the effects of the clashing μ-meson beams *JINR Report P2-4120* arXiv:0805.3961 (in Russian)
[55] Budker G I 1970 Accelerators and colliding beams *Proc. of the 7th Int. Conf. on High-energy Accelerators. (HEACC 1969), 27 August—2 September 1969, Yerevan, USSR* vol 1 pp 33–9
[56] Skrinsky A N and Parkhomchuk V V 1981 Cooling methods for beams of charged particles *Sov. J. Part. Nucl.* **12** 223 (in Russian) [Fiz. Elem. Chast. Atom. Yadra **12**, 557 (1981)]
[57] Neuffer D 1983 Principles and applications of muon cooling *Proc. of the 12 Int. Conf. on High Energy Accelerators (HEACC 1983), Fermilab, Batavia, USA. 11-16 August 1983. Conf. Proc. C* vol 830811, pp 481–4
[58] Blondel A, Ellis J R and Autin B 1999 Prospective study of muon storage rings at CERN *CERN Yellow Reports: Monographs* (Geneva Switzerland: CERN)
[59] Buttazzo D, Franceschini R and Wulzer A 2021 Two paths towards precision at a very high energy lepton collider *J. High Energy Phys.* JHEP05(2021)219
[60] Long K R, Lucchesi D, Palmer M A, Pastrone N, Schulte D and Shiltsev V 2021 Muon colliders to expand frontiers of particle physics *Nature Phys.* **17** 289
[61] Ankenbrandt C M, Atac M, Autin B, Balbekov V I and Barger V D 1999 Status of muon collider research and development and future plans *Phys. Rev. ST Accel. Beams* **2** 081001
[62] Delahaye J P *et al* (Muon Collider Working Group) Muon colliders arXiv:1901.06150
[63] Boscolo M *et al* 2018 Low emittance muon accelerator studies with production from positrons on target *Phys. Rev. Accel. Beams* **21** 061005
[64] Boscolo M, Delahaye J P and Palmer M 2019 The future prospects of muon colliders and neutrino factories *Rev. Accel. Sci. Tech.* **10** 189
[65] Bartosik N 2020 Detector and physics performance at a muon collider *JINST* **15** P05001
[66] Collamati F *et al* 2021 Advanced assessment of beam-induced background at a muon collider *JINST* **16** P11009
[67] Barger V, Berger M S, Gunion J F and Han T 1997 Higgs boson physics in the *s*-channel at $\mu^+\mu^-$ colliders *Phys. Rep.* **286** 1
[68] Chiesa M 2020 Measuring the quartic Higgs self-coupling at a multi-TeV muon collider *J. High Energy Phys.* JHEP09(2020)098
[69] Franceschini R and Greco M 2021 Higgs and BSM physics at the future muon collider *Symmetry* **13** 851
[70] Bandyopadhyay P and Costantini A 2021 Obscure Higgs boson at colliders *Phys. Rev.* D **103** 015025
[71] Han T, Liu D, Low I and Wang X 2021 Electroweak couplings of the Higgs boson at a multi-TeV muon collider *Phys. Rev.* D **103** 013002
[72] Han T, Li S, Su S, Su W and Wu Y 2021 Heavy Higgs bosons in 2HDM at a muon collider *Phys. Rev.* D **104** 055029
[73] Costantini A (New) physics at a multi-TeV μ collider arXiv:2111.02507
[74] Capdevilla R, Meloni F, Simoniellod R and Zurita J 2021 Hunting wino and higgsino dark matter at the muon collider with disappearing tracks *J. High Energy Phys.* JHEP06(2021)133
[75] Han T, Liu Z, Wang L-T and Wang X 2021 WIMPs at high energy muon colliders *Phys. Rev.* D **103** 075004
[76] Costantini A *et al* 2020 Vector boson fusion at multi-TeV muon colliders *J. High Energy Phys.* JHEP09(2020)080
[77] Asadi P, Capdevilla R, Cesarotti C and Homiller S 2021 Searching for leptoquarks at future muon colliders *J. High Energy Phys.* JHEP10(2021)182
[78] Bossi F and Ciafaloni P 2020 Lepton flavor violation at muon-electron colliders *J. High Energy Phys.* JHEP10(2020)033
[79] Capdevilla R, Curtin D, Kahn Y and Krnjaic G 2021 Discovering the physics of $(g-2)_\mu$ at future muon colliders *Phys. Rev.* D **103** 075028
[80] Jikia G and Tkabladze A 1994 Photon-photon scattering at the photon linear collider *Phys. Lett.* B **323** 453
[81] Gounaris G J, Porfyriadis P I and Renard F M 1999 Light-by-light scattering at high energy: a tool to reveal new particles *Phys. Lett.* B **452** 76
[82] Gounaris G J, Porfyriadis P I and Renard F M 1999 The $\gamma\gamma\to\gamma\gamma$ process in the standard and SUSY models at high energies *Eur. Phys. J.* C **9** 673
[83] Atağ S, İnan S C and Şahin İ 2010 Extra dimensions in $\gamma\gamma\to\gamma\gamma$ process at the CERN-LHC *J. High Energy Phys.* JHEP09(2010)042

[84] Gounaris G J, Layssac J, Porfyriadis P I and Renard F M 1999 The $\gamma\gamma \to \gamma Z$ process at high energies and the search for virtual SUSY effects *Eur. Phys. J.* C **10** 499

[85] Gounaris G J, Layssac J, Porfyriadis P I and Renard F M 2000 The $\gamma\gamma \to ZZ$ process and the search for virtual SUSY effects at a $\gamma\gamma$ collider *Eur. Phys. J.* C **13** 79

[86] Weizsäcker C F 1934 Ausstrahlung bei Stößen sehr schneller Elektronen *Z. Phys.* **88** 612

[87] Williams E J 1934 Nature of the high energy particles of penetrating radiation and status of ionization and radiation formulae *Phys. Rev.* **45** 729

[88] Brodsky S J 1971 Two-photon mechanism of particle production by high-energy colliding beams *Phys. Rev.* D **4** 1532

[89] Terazawa H 1973 Two-photon processes for particle production at high energies *Rev. Mod. Phys.* **45** 615

[90] Budnev V M, Ginzburg I F, Meledin G V and Serbo V G 1975 The two photon particle production mechanism. physical problems. applications. equivalent photon approximation *Phys. Rep.* **15** 181

[91] Carimalo C, Kessler P and Parisi J 1979 Validity of the equivalent-photon approximation for virtual photon-photon collisions *Phys. Rev.* D **20** 1057

[92] Dawson S 1985 The effective *W approximation Nucl. Phys.* B **249** 42

[93] Kane G L, Repko W W and Rolnick W B 1984 The effective $W^{\pm}$, Z^0 approximation for high energy collisions *Phys. Lett.* B **148** 367

[94] Cahn R N and Dawson S 1984 Production of very massive Higgs bosons *Phys. Lett.* B **136** 196 [Erratum-ibid. B **138**, 464 (1984)]

[95] Cahn R N 1985 Production of heavy Higgs bosons: comparisons of exact and approximate results *Nucl. Phys.* B **255** 341 [Erratum-ibid. B **262**, 744 (1985)]

[96] Lindfors J 1985 Distribution functions for heavy vector bosons inside colliding particle beams *Z. Phys.* C **28** 427

[97] Gunion J F, Kalinowski J and Tofighi-Niaki A 1986 Exact calculation of $ff \to ffWW$ for the charged-current sector and comparison with the effective-*W approximation Phys. Rev. Lett.* **57** 2351

[98] Altarelli G, Mele B and Pitolli F 1987 Heavy Higgs production at future colliders *Nucl. Phys.* B **287** 205

[99] Lindfors J 1987 Luminosity functions for $W^{\pm}$ and Z^0 initiated processes *Z. Phys.* C **35** 355

[100] Johnson P W, Olness F I and Tung W-K 1987 Effective-vector-boson method for high-energy collisions *Phys. Rev.* D **36** 291

[101] Kuss I and Spiesberger H 1996 Luminosities for vector-boson-vector-boson scattering at high energy colliders *Phys. Rev.* D **53** 6078

[102] Ruiz R, Costantini A, Maltoni F and Mattelaer O 2022 The effective vector boson approximation in high-energy muon collisions *J. High Energy Phys.* JHEP06(2022)114

[103] Greco M 2016 ISR effects for resonant Higgs production at future lepton colliders *Phys. Lett.* **763** 409

[104] Cowan G, Cranmer K, Gross E and Vitells O 2011 Asymptotic formulae for likelihood-based tests of new physics *Eur. Phys. J.* **71** 1554 [Erratum *ibid*. **73**, 2501 (2013)]C

[105] Dolan M J *et al* 2017 Revised constraints and Belle II sensitivity for visible and invisible axion-like particles *J. High Energy Phys.* JHEP12(2017)094

[106] Jacob M and Wick G C 1959 On the general theory of collisions for particles with spin *Ann. Phys. (N.Y.)* **7** 404

Jacob M and Wick G C 2000 On the general theory of collisions for particles with spin *Ann. Phys.* **281** 774

[107] Wigner E P 1959 *Group Theory and Its Application to The Quantum Mechanics of Atomic Spectra* (New York: Academic Press)

[108] İnan S C and Kisselev A V 2021 Probing anomalous $\gamma\gamma\gamma Z$ couplings through γZ production in $\gamma\gamma$ collisions at the CLIC *J. High Energy Phys.* JHEP10(2021)121

[109] Erdélyi A *et al* (ed) 1953 *Higher Transcendental Functions* vol 1 (New York: McGraw-Hill)

[110] Erdélyi A (ed) 1953 *Higher Transcendental Functions* vol 2 (New York: McGraw-Hill)

[111] Prudnikov A P, Brychkov Y A and Marichev O I 1989 Integrals and series *More Special Functions* (New York: Gordon & Breach Science Publishers) vol 3